Supporting Information: Solution-Phase Conformational/Vibrational Anharmonicity in Co-Monomer Incorporation Polyolefin Catalysis

James J. Lawniczak,[†] Xinglong Zhang,[†] Matthew Christianson,[‡] Brad Bailey,[‡] Sean Bremer,[‡] Sarah Barcia,[¶] Sukrit Mukhopadhyay,[‡] Jerzy Klosin,[‡] and Thomas F. Miller III[*,†]

[†]*Division of Chemistry and Chemical Engineering, California Institute of Technology, Pasadena, CA 91125, USA*

[‡]*The Dow Chemical Company, Midland, MI 48674, USA*

[¶]*Kelly Services, Inc., Troy, MI 48084, USA*

E-mail: tfm@caltech.edu

Structural Data

All structures are provided in the attached .zip folders, containing the monomer-bound and insertion-product catalyst structures. For the resting state form which omits the monomer, Catalyst CGC-A is (*tert*-butyl(dimethyl-η^5-(2,3,4,5-tetramethylcyclopenta-1,3-dienyl)silyl) amido)(propyl)titanium(IV), CGC-B is [1-[(1,2,3,3a,11b-η)-1H-cyclopenta[l]phenanthren-2-yl]-*N*-(1,1-dimethylethyl)-1,1-dimethylsilanaminato(2-)-κN]-titanium, and CGC-C is (*N*-(1,1-dimethylethyl)-1,1-dimethyl-1-((1,2,3,3a,7a-η)-3-(1-pyrrolidinyl)-1H-inden-1-yl)silanaminoato(2-)-N)titanium.

Coordination Number Parameterization

The coordination number $CN1$ is parameterized as $n = 15, m = 20, r = 3.5$ and coordination number $CN2$ is parameterized as $n = 15, m = 20, r = 2.1$.

QM/MM

Representative XML files for the QM/MM simulations are available in the supplemented .zip folder.

Statistical Error Determination

The statistical error for the insertion free energy barrier for a given system is computed with the following protocol. First, for each point on the ZTS, five different sets of gradients are obtained from five sequential segments of the MD trajectories. Five different free energy surfaces computed from each set of gradients obtained from a MD trajectory segment, and the variance is taken for the free energies at a fixed value of the collective variable. This approach evaluates the sensitivity of the total free energy barrier height to with respect to use of different segments of the MD trajectory.

Structural Analysis

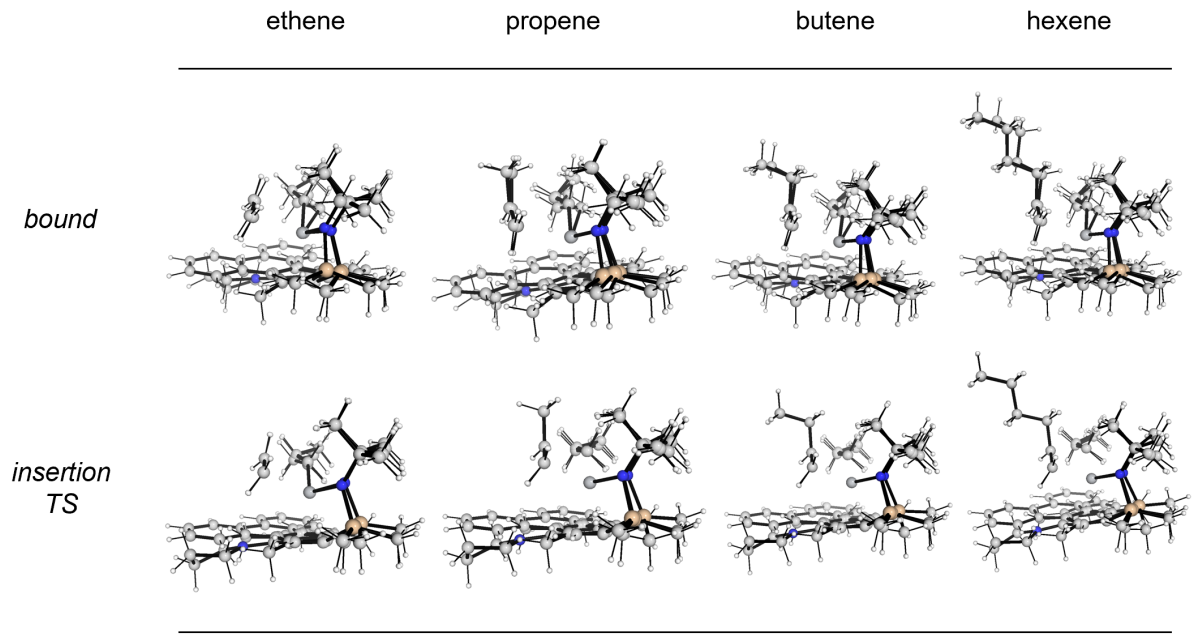

Figure 1. Structural overlap with respect to the monomer. For a given olefin monomer, the catalysts CGC-A, CGC-B, and CGC-C are overlayed for comparison. The orientation of the catalyst is consistent across all systems.

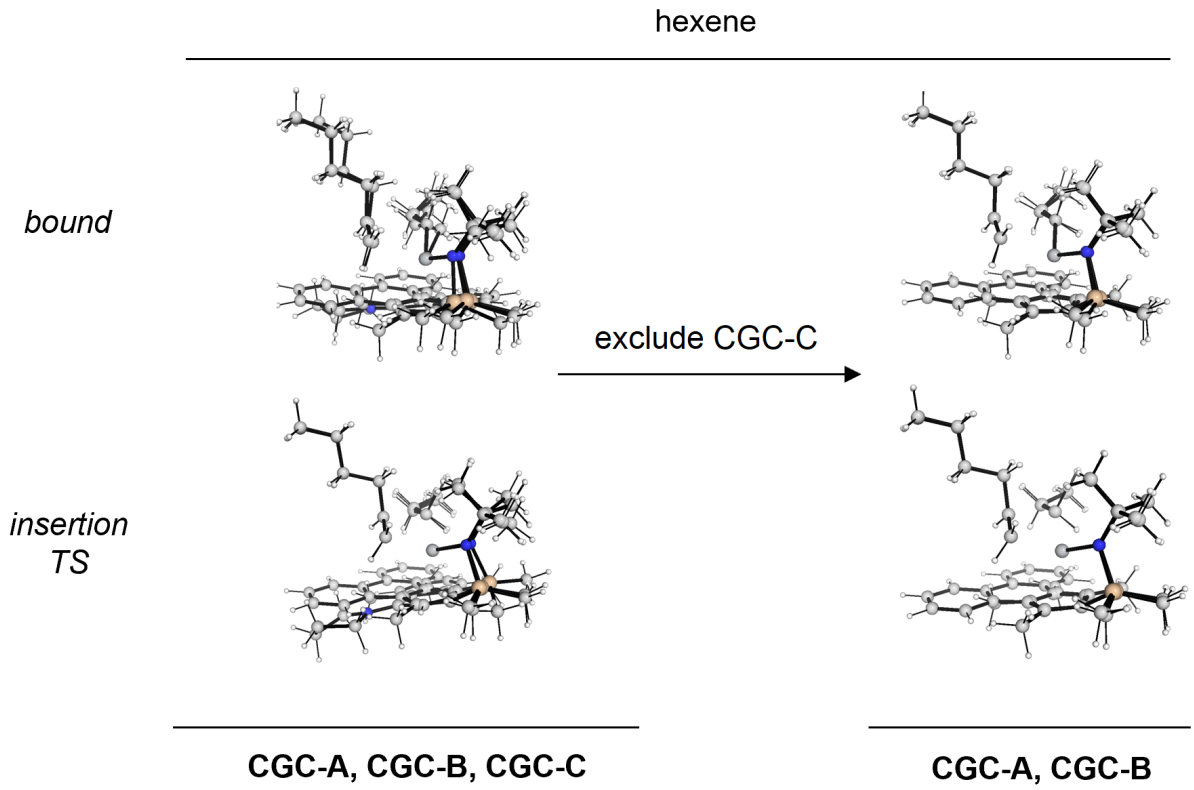

Figure 2. The bound and insertion TS structures involving the monomer hexene are overlapped in the left column. In the right column, removing the CGC-C catalyst and overlapping only the CGC-A and CGC-B structures reveals close correspondence in the structures. The unique geometry of the CGC-C structures reflects the bound monomer distorting the ligand scaffold.

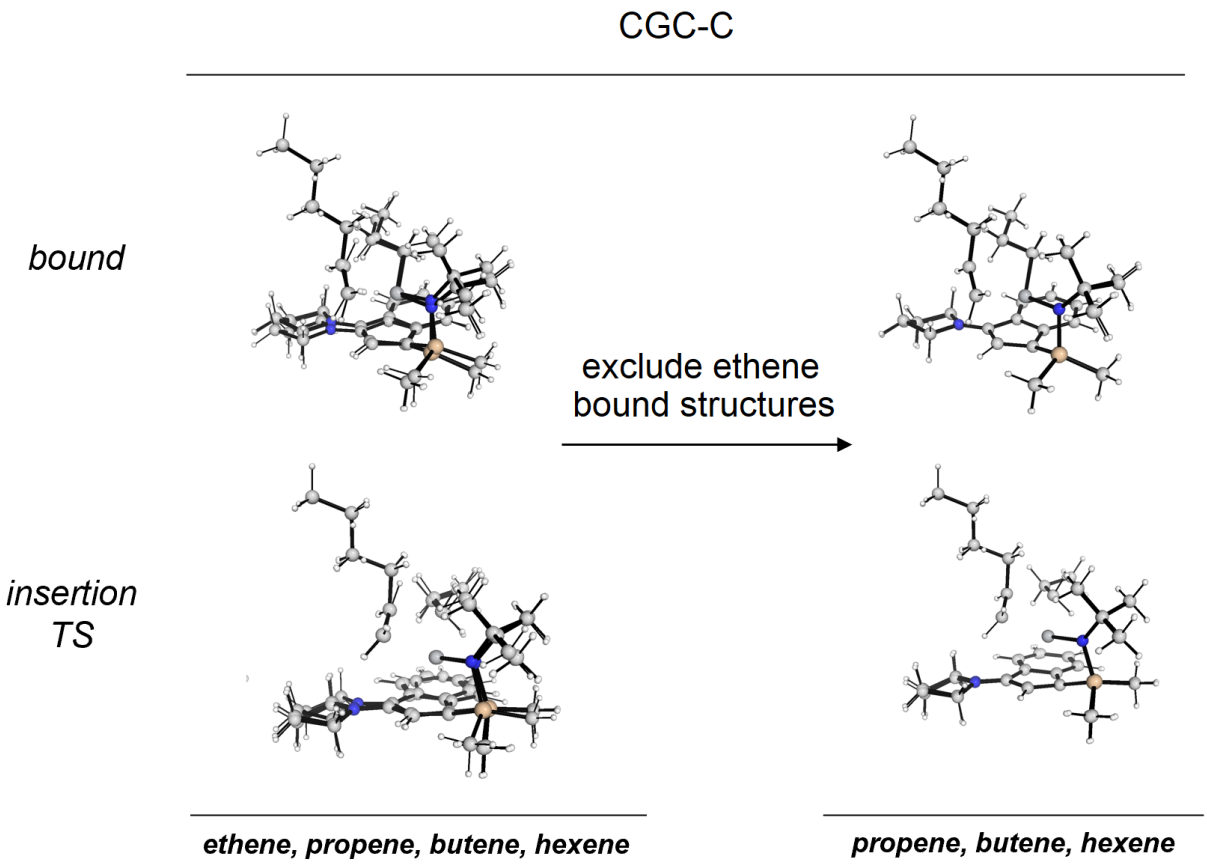

Figure 3. The bound and insertion TS involving catalyst CGC-C are overlapped in the left column. In the right column, removing the structures involving the monomer ethene and overlapping only the structures with propene, butene, and hexene monomers reveals close correspondence in the structures. The unique geometry of the structures involving ethene monomer reflects the decreased steric constraints of ethene, which lacks bulky substituents, relative to propene, butene, and hexene.

Free Energy Results

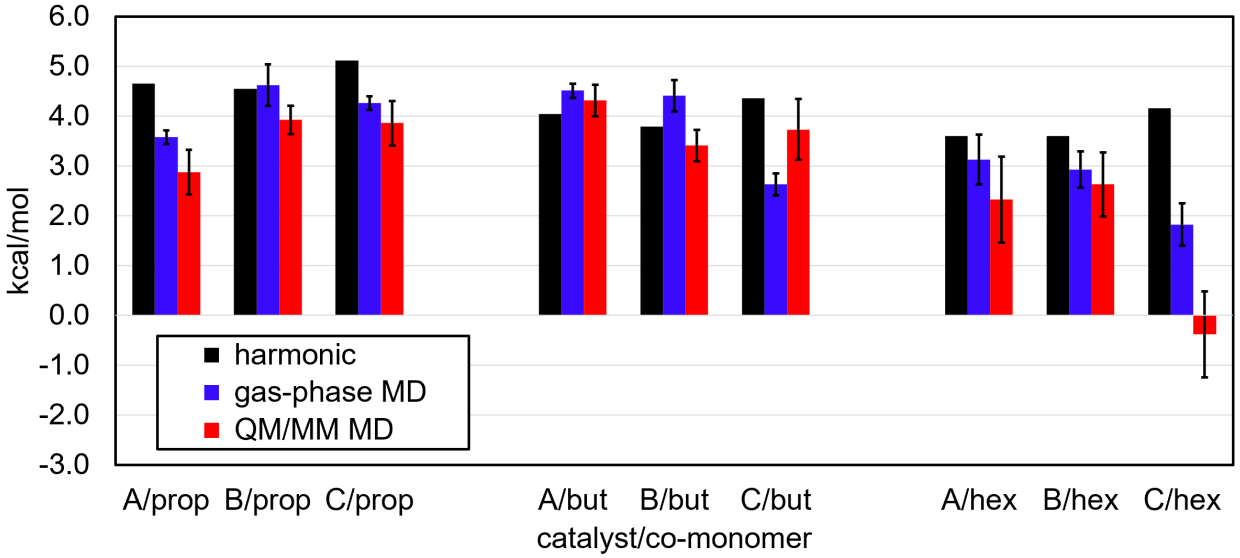

Figure 4. The insertion transition state energy difference ($\Delta\Delta G^{\ddagger}$) is computed using either the harmonic approximation (with implicit solvation correction) or sampling of restrained molecular dynamics trajectories.

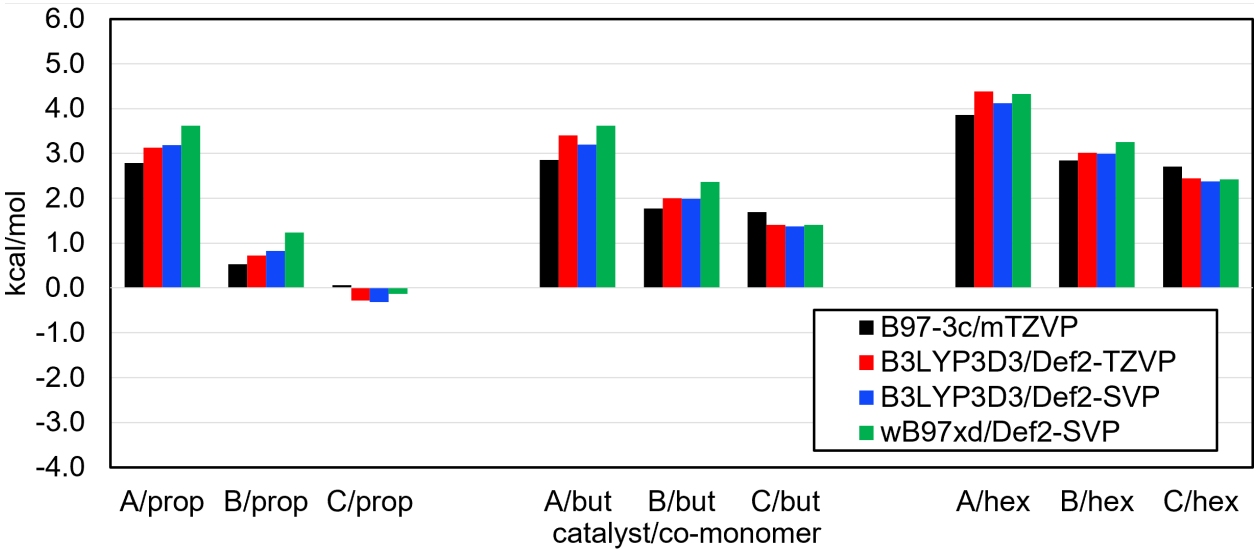

Figure 5. The monomer interconversion equilibrium (ΔG_{ce}) energies are computed across different DFT methods.

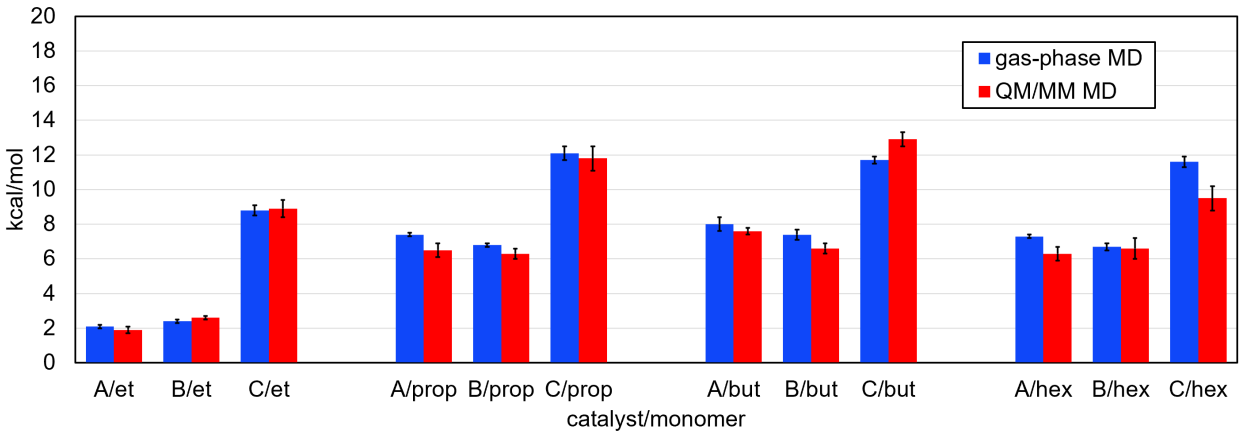

Figure 6. The insertion barrier heights ($\Delta G^{\ddagger}$) are computed using gas-phase and solution-phase MD sampling.

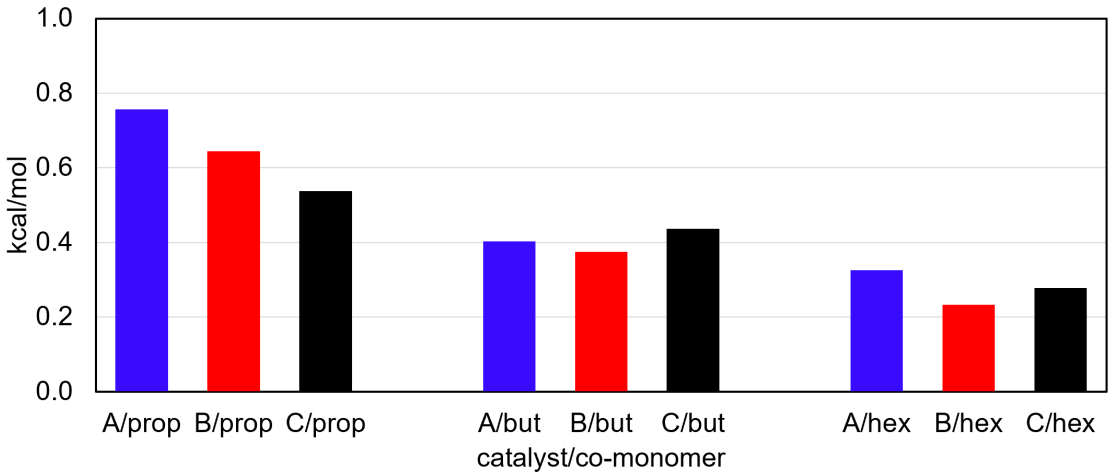

Figure 7. The zero-point energy corrections to the insertion BHDs are computed. In the main text, the harmonic correction to the free energies composes of the zero-point energy and thermal contributions.

Table 1: For linear olefin monomers with three or more carbons, two orientations involving the alkene substitution relative to the cyclopentadienyl ring are considered. Orientation A implies the alkene substitution points away from the cyclopentadienyl ring, and B implies the substitution points toward the ring. The static DFT (B97-3c/mTZVP) results for the insertion TS energy difference $\Delta\Delta G^{\ddagger}$ (kcal/mol units) are presented below for each monomer orientation. The static free energies take into account the implicit solvation correction. In the main text, orientation A is chosen for all systems.

System	$\Delta\Delta G^{\ddagger}_{A}$	$\Delta\Delta G^{\ddagger}_{B}$	$\Delta\Delta G^{\ddagger}_{A} - \Delta\Delta G^{\ddagger}_{B}$
CGC-A/propene	4.7	4.5	0.2
CGC-B/propene	4.5	4.8	−0.3
CGC-C/propene	5.1	4.2	0.9
CGC-A/butene	4.0	3.8	0.2
CGC-B/butene	3.8	4.1	−0.3
CGC-C/butene	4.4	4.1	0.3
CGC-A/hexene	3.6	3.0	0.6
CGC-B/hexene	3.6	4.3	−0.7
CGC-C/hexene	4.2	3.6	0.6

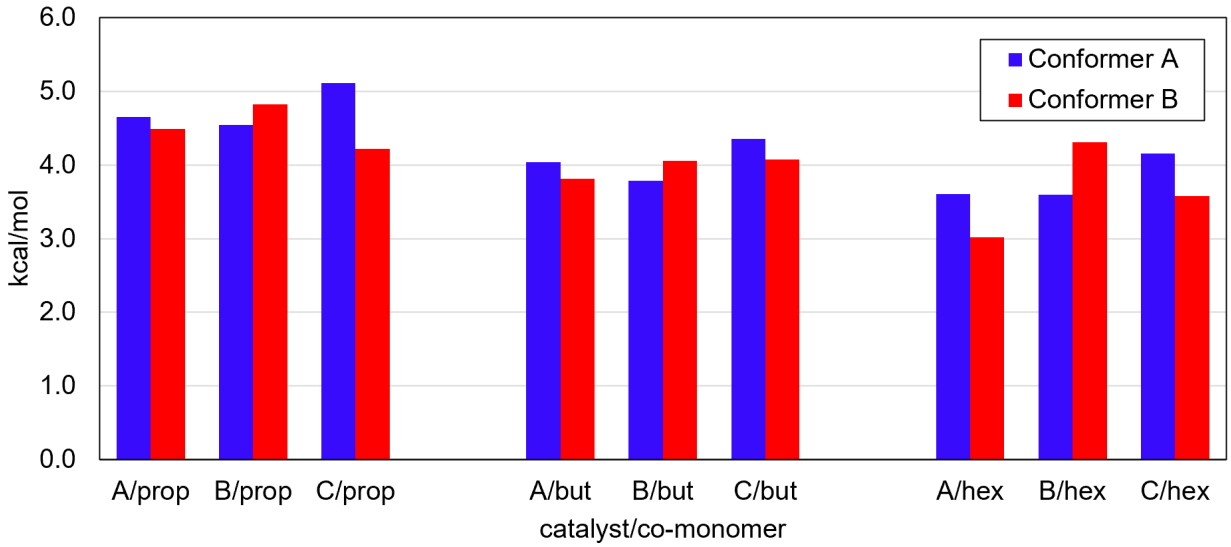

Figure 8. The insertion TS energy difference $\Delta\Delta G^{\ddagger}$ (kcal/mol units) are presented for each monomer orientation A and B (see Table 1).

Assessment of Simulation Convergence

To assess the convergence of the free energy gradients, the CN2 collective variable (monomer insertion) is displayed below in Figure 9 for each MD run and each system. A given MD run corresponds to a restraint on the CN2 collective variable (blue line), and the average value of the CN2 variable at a given time (red line) is observed for convergence.

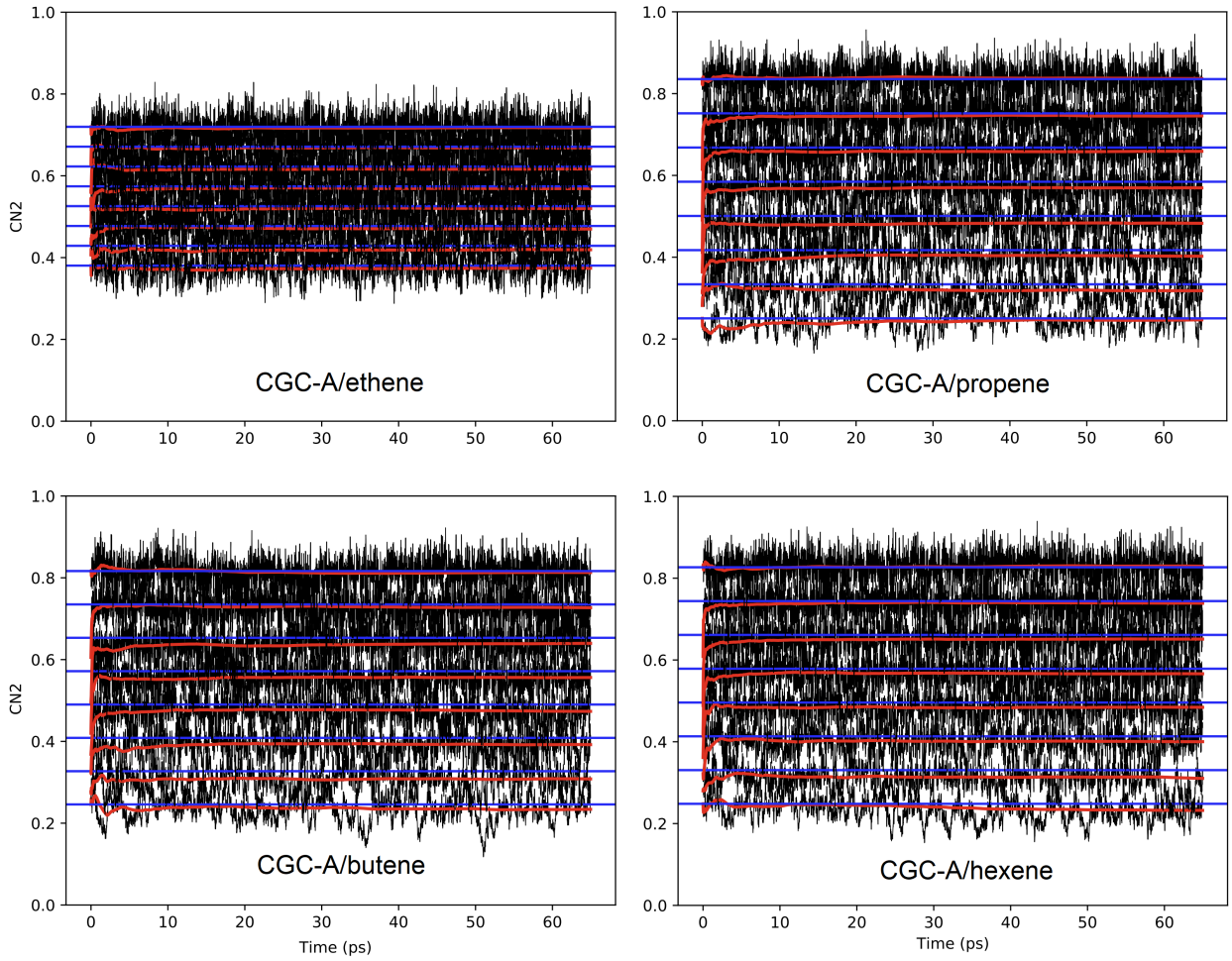

Figure 9. Convergence plots for the CN2 collective variable are shown for each trajectory corresponding to CGC-A. For a given trajectory, the black line denotes the value of CN2, the blue line denotes the restraint value, and the red line is the cumulative average of CN2.

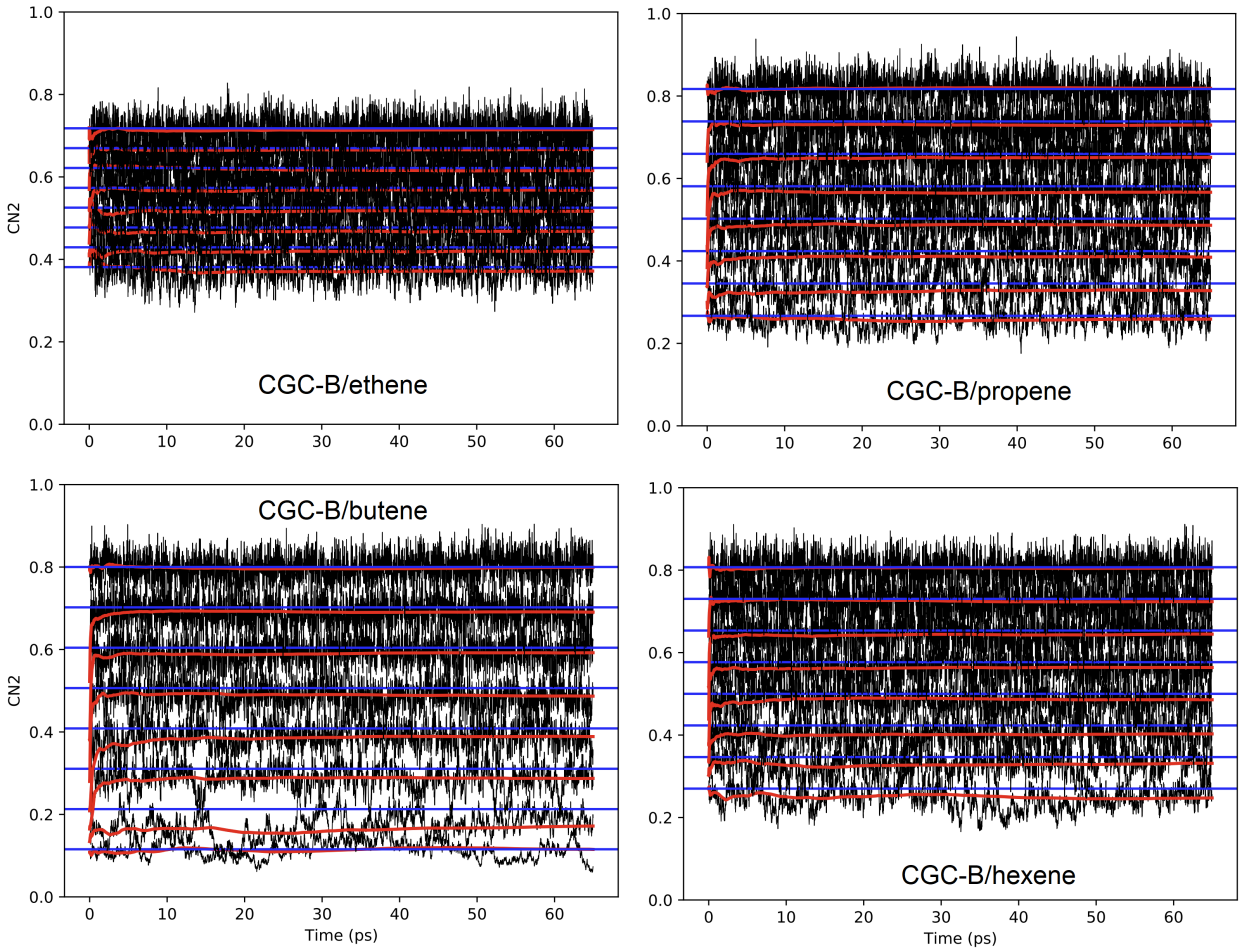

Figure 10. Convergence plots for the CN2 collective variable are shown for each trajectory corresponding to CGC-B. For a given trajectory, the black line denotes the value of CN2, the blue line denotes the restraint value, and the red line is the cumulative average of CN2.

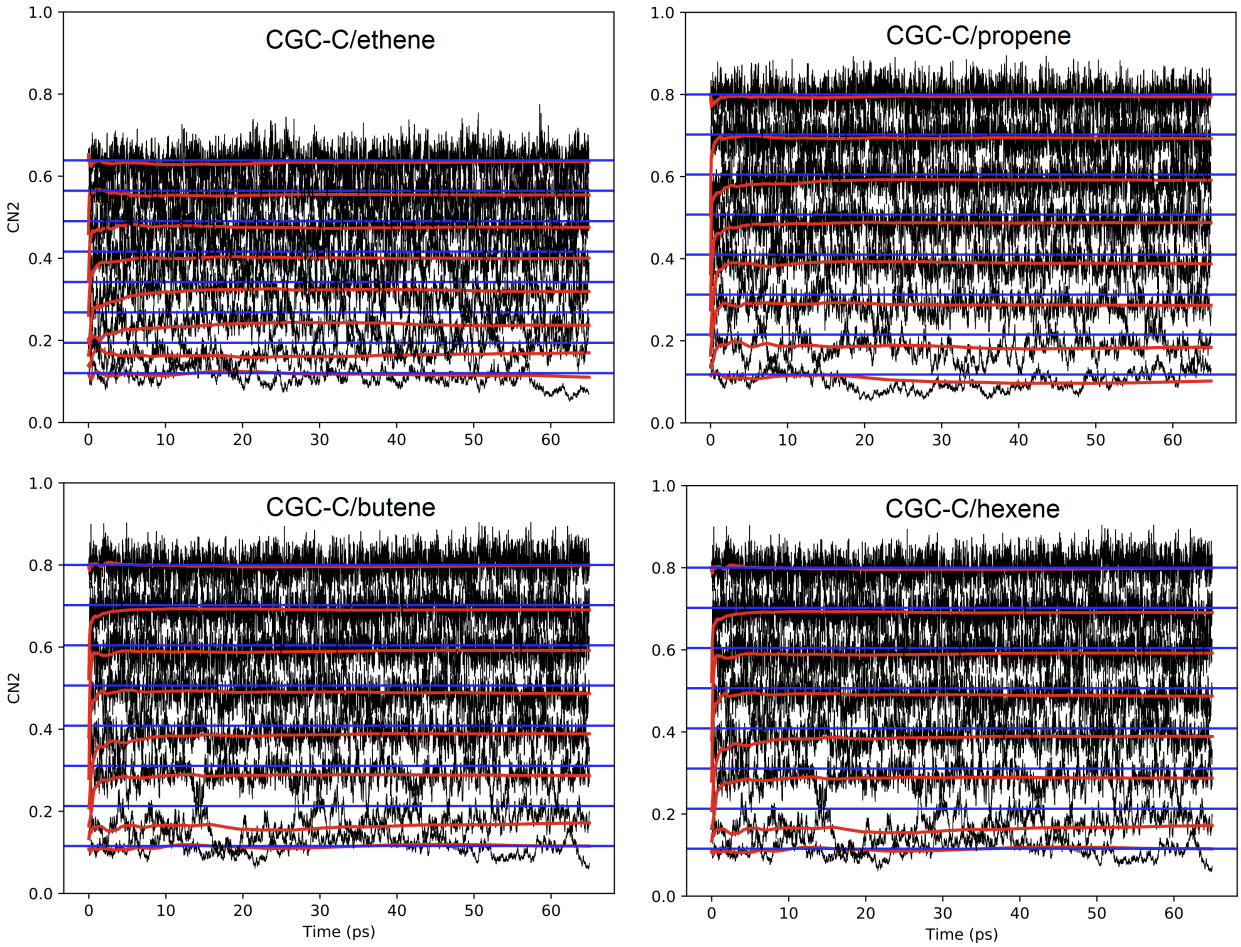

Figure 11. Convergence plots for the CN2 collective variable are shown for each trajectory corresponding to CGC-C. For a given trajectory, the black line denotes the value of CN2, the blue line denotes the restraint value, and the red line is the cumulative average of CN2.

Details of Polymerization Reactor Runs

Table 2: Conditions for running the semi-batch reactor runs; for all the runs, 10 μmol of MMAO-3A was used as scavenger, octene was used as comonomer, isopar E was used as solvent and the reactor was run for 10 mins at 120 °C with FAB ($B(C_6F_5)_3$) and RIBS-II ($[HNMe(C_{13}H_{27})_2][B(C_6F_5)_4]$) as activators. 40 mg of each anti-oxidants (pentaerythritol tetrakis(3,5-di-*tert*-butyl-4-hydroxyhydrocinnamate) and tris(2,4-di-*tert*-butylphenyl) phosphite) are added after each polymerization run.

#	Catalyst	Catalyst loading (μmol)	Activator	Activator loading (μmol)	Isopar loading (g)	Ethene loading (g)	Octene loading (g)	Reactor pressure (kPa)
1	CGC-A	0.25	RIBS-II	0.30	611.1	46.2	301.6	2003
2	CGC-A	0.25	FAB	0.75	611.3	46.3	301.7	2013
3	CGC-C	0.15	RIBS-II	0.18	611.2	46.3	302.0	1864
4	CGC-C	0.15	FAB	0.45	612.0	46.3	303.3	1906

Table 3: Reactor output for all the semi-batch reactor runs.

#	Catalyst	Ethene uptake (g)	Exotherm (°C)	Polymer yield (g)
1	CGC-A	16.2	1.7	70.2
2	CGC-A	12.3	1.9	47.1
3	CGC-C	9.3	13.0	78.5
4	CGC-C	12.4	14.0	57.1

Table 4: Polymerization data for all the semi-batch reactor runs; the efficiency of the catalysts is reported as g of polymer/g of metal.

#	Catalyst	Efficiency	T_g (°C)	T_m (°C)	M_w (g/mol)	PDI	octene wt%	octene mol%
1	CGC-A	5,864,662	-67.3	−26.3	42,004	2.4	60.2	27.4
2	CGC-A	3,934,837	-66.4	−22.9	39,499	2.3	59.9	27.2
3	CGC-C	10,930,103	-64.9	53.5	216,256	2.8	46.0	17.6
4	CGC-C	7,950,432	-58.8	51.4	244,413	2.4	39.8	14.2

Based on Table 4, the experimental $\Delta\Delta G^{\ddagger}$ (kcal/mol) are computed based on the following formulae, using 0.72 mol/L and 1.67 mol/L for ethene and octene concentrations, respectively:

$$\Delta\Delta G^{\ddagger} = RT \times \ln \frac{100 \times 1.67 - 1.67 \times (\text{mol \% octene})}{0.72 \times (\text{mol \% octene})} \tag{1}$$

$$r_c = \frac{30.1}{69.9} \times \frac{\text{mol \% octene}}{\text{mol \% ethene}} \tag{2}$$

Based on the above equation, the average $\Delta\Delta G^{\ddagger}$ for CGC-A was found to be 1.4 kcal/mol and for CGC-C was found to be 2.0 kcal/mol. The prefactor in Eq. 2 is computed by converting the mol/L value of ethene (0.72 mol/L) and octene (1.67 mol/L) to percentages. Based on Eq. 2, the average r_c for CGC-A is 0.17 and for CGC-C is 0.083.